Analyst

Accepted Manuscript

ROYAL SOCIETY OF CHEMISTRY

www.rsc.org/analyst

Cite this: DOI: 10.1039/c0xx00000x

www.rsc.org/xxxxxx

ARTICLE TYPE

Azodye−Rhodamine-Based Fluorescent and Colorimetric Probe Specific for the Detection of Pd^{2+} in Aqueous Ethanolic Solution: Synthesis, XRD characterization, Computational Studies and Imaging in Live Cells

Ajit Kumar Mahapatra*,[a] Saikat Kumar Manna,[a] Kalipada Maiti,[a] Sanchita Mondal,[a] Rajkishor Maji,[a] Debasish Mandal,[b] Sukhendu Mandal,[c] Md. Raihan Uddin,[c] Shyamaprosad Goswami,[a] Ching Kheng Quah[d] and Hoong-Kun Fun[d,e]

Received (in XXX, XXX) Xth XXXXXXXXX 20XX, Accepted Xth XXXXXXXXX 20XX
DOI: 10.1039/b000000x

Azodye–rhodamine hybrid colorimetric fluorescent probe (**L**) has been designed and synthesized. The structure of **L** has been established based on single crystal XRD. It has been shown to act as selective *turn-on* fluorescence chemosensor for Pd^{2+} with > 40 fold enhancement by exhibiting red emission among the other 27 cations studied in aqueous ethanol. The coordination features of the species of recognition have been computationally evaluated by DFT methods and found to have distorted tetrahedral Pd^{2+} center in the binding core. The probe (**L**) has been shown to detect Pd up to 0.45 μM at pH 7.4. Furthermore, the probe can be used to image Pd^{2+} in living cells.

Introduction

In recent years, platinum–palladium group elements are commonly used as efficient catalysts for carbon-carbon and carbon-heteroatom coupling transformation reactions.[1] These reactions have found increased popularity to build complicated pharmaceutical molecules. However, palladium-catalyzed reactions present a problem in that the residual palladium can often be retained in the isolated drug molecules (Active Pharmaceutical Ingredients).[2] Palladium influences our environment in an adverse way because Pd emission from automobile catalytic converters[3] has rapidly increased the Pd concentrations in diverse environmental matrices, such as soil and roadside dust,[4] plants,[5] rivers[6] and coastal and oceanic environments.[7] At the same time, palladium influences our health[8] because it can bind to thiol-containing amino acids, proteins (casein, silk fibroin and many enzymes), DNA or other macromolecules and biomolecules (vitamin B6)[9]. Therefore, it may disturb a variety of cellular processes when this heavy metal accumulates in the human body.[10] This issue raises the urgent need to develop effective sensing methods for palladium species in a sensitive and selective way in aqueous media.

Conventional analytical methods for palladium species include atomic absorption spectrometry (AAS), inductively coupled plasma mass spectrometry (ICP-MS), solid phase microextraction-high performance liquid chromatography, X-ray fluorescence, etc.[11] However, these methods often need serious sample-preparation steps, high cost of instrumentation and requirement of well-trained individuals. Thus, current research has been focused on fluorescent methods, because of their easy preparation and convenient operation, low cost, and sensitivity.[12] Pd^{2+} is a well-known fluorescence quencher due to its 'open-shell' electronic configuration and heavy transition-metal ion.[13] However, a fluorescence-enhanced chemosensor would be more desirable for Pd^{2+} detection. Holdt *et al.* designed the first chemosensor for Pd^{2+} detection by increasing fluorescence.[14] Some fluorescent chemosensors[15] and chemodosimeters[16] based on the ON–OFF [17] or OFF–ON[18] mechanism for the palladium species have been reported in the literature recently. Peng and co-workers have modified the spirolactam moiety with suitable ligands to develop fluorescence-enhanced palladium probes, which have satisfactory sensitivity, selectivity, and response time.[19]

Practically, OFF–ON fluorescence signal is more reliable than an ON–OFF signal. In this regard, the rhodamine platform has been widely exploited to construct off−on fluorescence probes because in rhodamine framework contains spirolactam (non-fluorescent) to ring open amide (fluorescent) equilibrium, [20] during the

identification of metal ions.[21] In this study, a novel rhodamine-azo-based derivative as the fluorescence sensor for the detection of Pd^{2+} and that can selectively detect Pd^{2+} (0–20 mM) over other examined metal ions studied in aqueous solution. This probe was based on coordination reaction. Here, Pd^{2+} ions can coordinate with the probe core which contains O, N and O binding centres and this can lead to a change in the color and fluorescence of the probe.

The recognition of **L** to Pd^{2+} is based on the Pd^{2+} induced opening of the well-known nonfluorescent colorless spirolactam-ring of rhodamine. The Pd complexation induces the ring to open, leading to a brilliant pink color and emitting strong fluorescence of the rhodamine dye. The probe has high selectivity for Pd^{2+} among the metal ions (including the platinum-group metal ions).

Results and discussion

The chemosensor molecule, **L** has been synthesized in a single step on rhodamine platform by reacting rhodamine B hydrazide with azo-couple salicylaldehyde(**2**)[22] in 85% yield (Scheme 1) and the structure of **L** was well characterized by ^{1}H NMR, ^{13}C NMR, FTIR, ESI-MS and by single–crystal X-ray diffraction analysis (Fig. S1-S3 and S5†). The **L**-Pd^{2+} complex were characterized by ESI-MS and FTIR analysis (Fig. S4 and S5†).

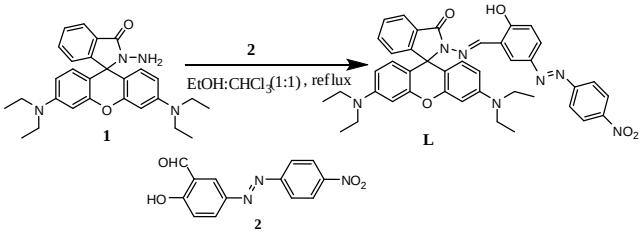

Scheme 1 The synthetic procedure of sensor **L.**

A reddish yellow colored single crystal[‡] of this probe **L** was obtained by slow evaporation of the solvent from a solution in EtOH/$CHCl_3$ (1:1). It crystallizes as triclinic with space group *P*1.

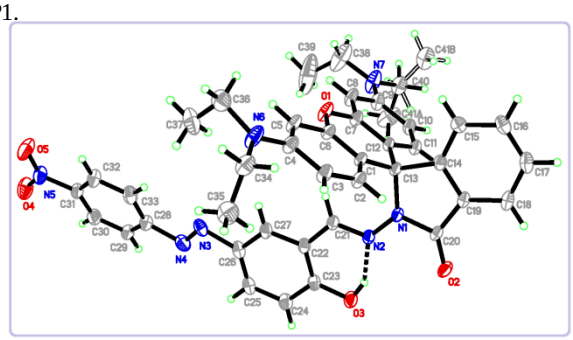

Fig. 1 The molecular structure of **L**, showing 30% probability displacement ellipsoids for non-H atoms and the atom-numbering scheme. An intramolecular hydrogen bond is indicated as a black dashed line.

The corresponding details of the structure determination and refinement data are given in Table S1 (ESI†). The probe **L** (Fig. 1) exists in a *trans* conformation with respect to the N3=N4 bond and their corresponding bond length 1.196(5) Å. The crystal structure is stabilized by an intramolecular O3–H1···N2 hydrogen bond, forming S(6) ring motif. One of the methyl groups is disordered over two positions with refined site-occupancies of 0.550(13) and 0.450(13). The xanthene ring system (O1/C1-C13) is essentially planar (*r.m.s.* deviation = 0.023 Å) and it forms dihedral angles of 88.18(10), 82.91(15) and 59.75(18)° with the isoindoline ring system (N1/C13-C20, *r.m.s.* deviation = 0.023 Å) and two benzene rings (C22-C27 and C28-C33), respectively. The C22-C27 and C28-C33 benzene rings incline at dihedral angles of 11.80(15) and 34.82(18)°, respectively, to the isoindoline ring system whereas the dihedral angle between the two benzene rings is 23.9(2)°.

In the crystal packing (Fig. 2), the molecules are linked together as dimers *via* pairs of intermolecular C11—H11*A*···O2 hydrogen bonds and stacked along the a-axis. The crystal structure is further consolidated by C21—H21A ···π interactions which involves the 4H-pyran ring (Table S2†).

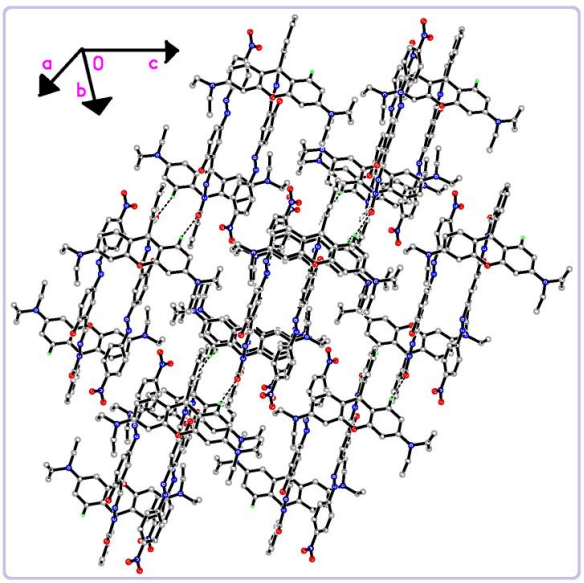

Fig. 2 The crystal packing of **L** viewed along the *a* axis. H atoms not involved in intermolecular interactions (dashed lines) have been omitted for clarity.

In order to ascertain the complexation of Pd^{2+} by **L**, absorption titrations were carried out by adding varying concentrations of Pd^{2+} to a fixed concentration of **L**. The free **L** exhibits three weak bands at 276, 317 and 384 nm. Upon the addition of Pd^{2+}, the absorbance at 276, 317 and 384 nm decreases and that at 561 nm increases as a function of the increase in [Pd^{2+}] (Fig. 3) and leads to a brilliant pink coloration. The isosbestic point observed at 401 nm clearly indicate that the transition between the free and the complexed species occurs, while the other metal ions exhibit no significant change in the absorption spectra (ESI†). The stoichiometry of the complex formed between **L** and Pd^{2+} is 1:1 based on Job's plot (Fig. S6†). The result was also confirmed through ESIMS analysis, and it is well matched with theoretical mass spectral simulation. The peak at m/z 873.1252 in the mass spectrum is assignable to the mass of [**L** + Pd^{2+}+ Cl^-]$^+$ (Fig. S4†).

Therefore, we suggest that probe **L** coordinates with Pd^{2+} with 1:1 stoichiometry. The mass spectra of [**L** + Pd^{2+}]$^+$ also appeared at m/z 814.0356. The detection limit (LOD) was measured to be 0.45 μM level by the naked eye in aqueous ethanolic solution (Fig. S7†).

In order to find suitable solvent system of **L** to sense Pd^{2+} in aqueous buffer solution at physiological pH, fluorescence titrations were carried out in 10 mM aqueous HEPES buffer taken with ethanol in a volume to volume ratio of 1 : 1 at pH = 7.4 to give an effective sensing only for Pd^{2+}. All the other metal ions, viz., Li^+, Na^+, K^+, Sr^{2+}, Ba^{2+}, Mg^{2+}, Ca^{2+}, Cr^{3+}, Mn^{2+}, Fe^{2+}, Fe^{3+}, Co^{2+}, Ni^{2+}, Pd^0, Pt^{2+}, Cu^{2+}, Zn^{2+}, Cd^{2+}, Hg^{2+}, Pb^{2+}, Ag^+, Al^{3+}, Ru^{3+}, Au^{3+} , Zr^{4+}, Hf^{4+} and Sn^{4+} used in the titrations do not show the development of a new band at 579 nm, which was present only in the case of Pd^{2+} in aqueous ethanolic buffer-medium.

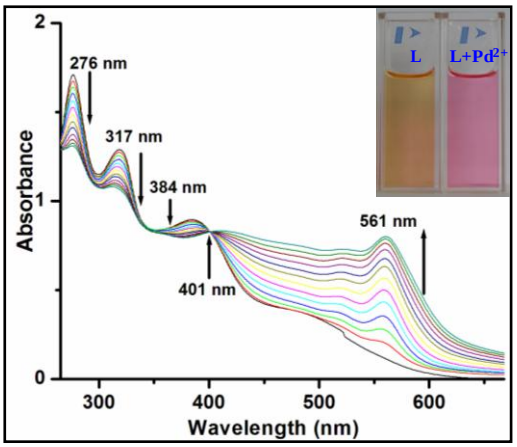

Fig. 3 UV-Vis spectral changes of sensor **L** (c = 4× 10^{-5} M) in EtOH/H_2O (1:1, v/v, 10 mM HEPES buffer, pH 7.4) solutions upon addition of Pd^{2+} ions (0-1 equivalent) (c = 1× 10^{-4} M) in EtOH/ H_2O (1:1, v/v) at pH 7.4. Inset: The photographs showed the color change of **L** in the presence of Pd^{2+} ions.

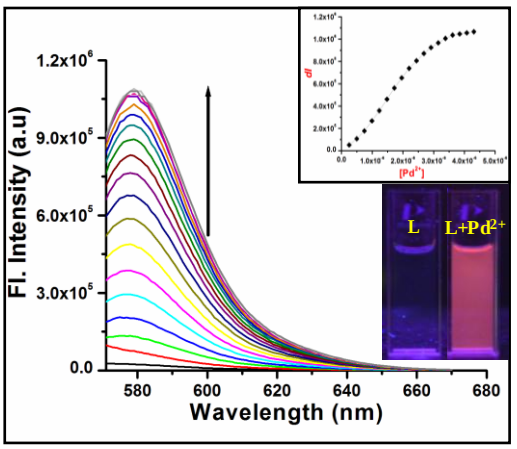

Fig. 4 Fluorescence emission changes of **L** (c = 4× 10^{-5} M) upon addition of Pd^{2+} ions (c = 1× 10^{-4} M) in EtOH/ H_2O (1:1, v/v) at pH 7.4 (λ_{ext}=561 nm). Inset: Fluorescence emission color changes of the receptor **L** solution on addition of Pd^{2+} ions and change of emission intensity at 579 nm with incremental addition of Pd^{2+} ions [λ_{ext}=561nm].

The chemosensor **L** exhibit no emission at 579 nm when excited at 561 nm in 1:1 water/ethanol mixture at pH 7.4 to have an effective HEPES buffer concentration of 10 mM. The absence of red fluorescence in the emission spectra 579 nm indicated a spirolactam ring-closed form of the rhodamine moiety in the metal-free solution of the probe. The spirolactam ring of the rhodamine moiety is susceptible to the changes in the pH; pH promotes ring-opening in the rhodamine and leads to emission of red fluorescence. Therefore, the near-neutral EtOH/H_2O (1:1, v/v) system was used in the subsequent assays.

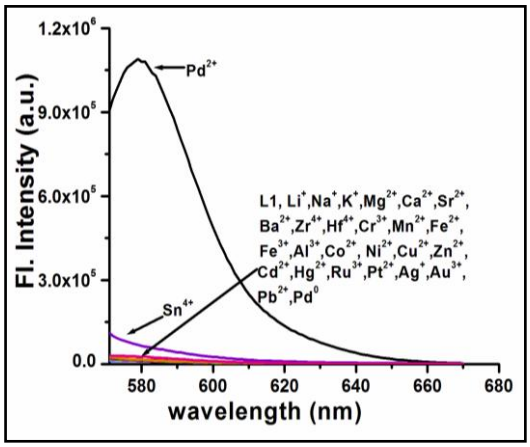

Fig. 5 Fluorescence responses of **L** to various metal ions in ethanol/H_2O (1:1, v/v, 10 mM HEPES buffer, pH 7.4).

Titration of **L** with Pd^{2+} results in the enhancement (up to 45-fold enhancement) of fluorescence intensity at 579 nm as a function of the added Pd^{2+} concentration (Fig. 4), suggesting a sensitive and selective recognition of Pd^{2+} by **L** when compared to all other metal ions studied (Fig. 5). The fluorescence intensities are linearly proportional to the amount of Pd^{2+} in the range of 0–4 ppm (Fig 4, inset). The chelation by Pd^{2+} to the imine N, phenolic O, and lactim O brings rigidity to the binding core and results in chelation-enhanced fluorescence (CHEF). During the chelation process, Pd^{2+} attached with O-N-O moieties and one chlorine atom resulting in a four-coordinated Pd^{2+} with a square planar geometry.[23] The Pd^{2+} sensing property of **L** has been further demonstrated by observing the visual fluorescent colors under a 365 nm lamp. A distinct color change was observed only in the case of Pd^{2+}, while no other metal ion exhibits such a change (Fig, S9 and S10†).

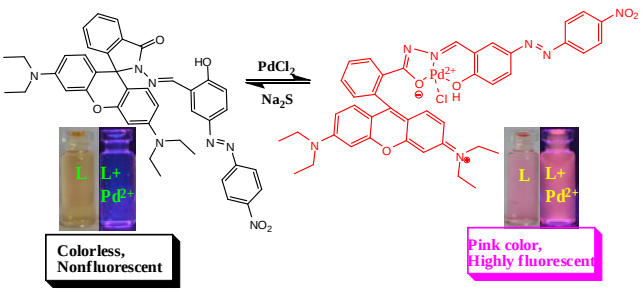

Scheme 2 Sensing of Pd^{2+} by ring opening of rhodamine spiro-lactam based probe **L**.

The binding affinities of Pd^{2+} toward **L** have been calculated from the Benesi−Hildebrand equation and found to have association constant $K_a = 1.7\times10^5$ (Fig. S11†).

Since the *in situ* generated [**L**-Pd] ensemble exhibits fluorescence enhancement, this is further subjected to the interaction by sulphide and Na_2EDTA, to determine the nature of the binding. With the increase in the concentration of sulphide or Na_2EDTA, the purple colored solution of [**L** -Pd] ensemble turned colorless and the fluorescence intensity at 579 nm disappeared (Fig. S12†) owing to decoordination of Pd. This phenomenon likely resulted from the removal of Pd^{2+} ion from **L**, leading to the reconstitution of the spirolactam ring in the rhodamine moiety and hence the loss of fluorescence at 579 nm. From these observations, the mechanism can be proposed in Scheme 2 for the detection of Pd^{2+} ions by **L**.

Pd^{2+} shows a remarkable change by showing fluorescence ON behavior by forming the [**L** -Pd] complex. Further titration of this with S^{2-} results in quenching of fluorescence and hence acts as an OFF switch. So, to examine whether the process is reversible, an excess of Na_2S was added to the solution containing [**L** -Pd] complex generated *in situ*. The bright fluorescence immediately turned off. This is due to the binding of S^{2-} ions to the [**L** -Pd] complex followed by the removal of Pd^{2+} in the form of PdS, thus releasing free **L**. The repeated demonstration of the ON/OFF behavior of fluorescence as well as visual color changes clearly suggest that **L** is a reversible and reusable sensor for Pd^{2+} followed by S^{2-} in a sequential manner (Fig. 6).

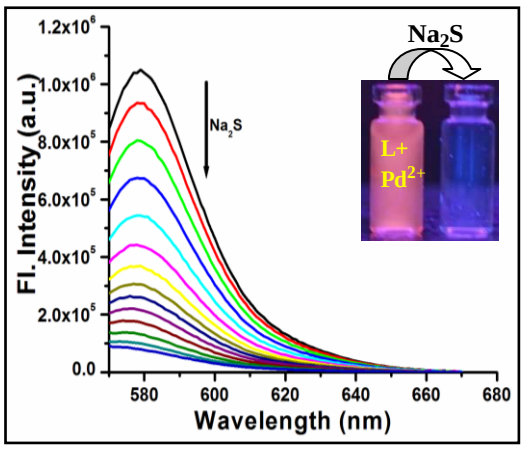

Fig. 6 Fluorescence emission changes of **L** ($c = 4\times10^{-5}$ M) with 1 equiv of Pd^{2+} ions upon addition of sodium sulfide ($c = 1\times10^{-4}$ M) in EtOH/ H_2O (1:1, v/v) at pH 7.4 (λ_{ext}=561 nm). Inset: fluorescence photographs of **L**-Pd complex after addition of Na_2S.

For practical applications, we have developed a colorimetric test kit for Pd^{2+} ion. The test kit was prepared by using TLC plates which were further immersed into the solution of **L** (4×10^{-4} M) in aqueous ethanol and then drying it by two ways (i) exposure to air and (ii) in vacuum. Next, to different Pd^{2+} concentration solutions, these strips were immersed and then exposed to air and in vacuum to evaporate the solvent. Fig. 7 exhibits the color changes of the TLC plates with different Pd^{2+} concentrations. When the Pd^{2+} ion concentration was increased, the color of the test strips changed from yellow to pink and it is easily differentiable by naked eyes. Therefore, the easy to-prepare test kit can be utilized to roughly and quantitatively detect and estimate the concentration of Pd^{2+} ions.

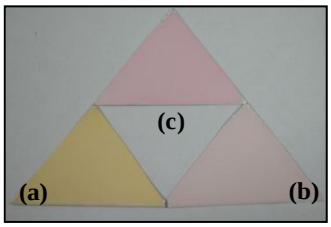

Under ambient light

Fig. 7 Photographs of Colorimetric test kits with **L** for the detection of Pd^{2+} ions in solution with different Pd^{2+} concentrations: (a) **L** (b) **L**+ Pd^{2+} (1×10^{-3} M) and (c) **L**+ Pd^{2+} (3×10^{-3} M).

Moreover, to explore potential and analytical applications of the chemosensor **L** for Pd^{2+} ions, we tested whether it could detect residual Pd in a reaction system. DMSO solution of $PdCl_2$ was stirred in a flask for 2 h at room temperature.

Fig. 8 Colorimetric photographs of residual Pd detection in reactors: (a) ethanolic solution of **L** in cleaned flask and (b) after overnight stirring at r.t.

After that, the flasks was cleaned by standard laboratory washing procedure (brushing with detergent, washing with water and acetone) and then ethanolic solution of **L** were added to the 'washed and cleaned' flasks and stirred overnight. The reaction flasks turned pink from light yellow color which can be detected by our naked eye (Fig. 8). It does not show obvious fluorometric and colorimetric responses towards Pd^0 $[Pd(PPh_3)_4]$-complexes. Therefore, this experiment demonstrated that the **L**-Pd^{2+} sensing method can be used for the quality control of reactors.

In order to understand the binding behavior of **L** with Pd^{2+}, the geometry optimizations for **L** and [**L**-Pd] complex (Fig. 9) were done in a cascade fashion starting from semiempirical PM2 followed by *ab initio* HF to DFT B3LYP[24] by using various basis sets, *viz.*, PM2 → HF/STO-3G → HF/3-21G → HF/ 6-31G → B3LYP/ 6-31G(*d,p*). In the optimized structure of [**L**-Pd], the **L** is bonded to the imine N, phenolic O, lactim O, and one chlorine atom resulting in a four-coordinated Pd^{2+} with a square planar geometry. Molecular Orbitals (MOs) were calculated using the B3LYP with LANL2DZ level.[25] The spatial distributions and orbital energies of HOMO and LUMO of **L** and [**L**-Pd] were also determined (Fig. 10).The HOMOs were majorly localized on

rhodamine part, though these were extended with the lactam-Schiff's base orbitals. The LUMOs are present on azo residues. Therefore, the computational studies further support the involvement of the lactim-imino-phenolic core in **L** binding.

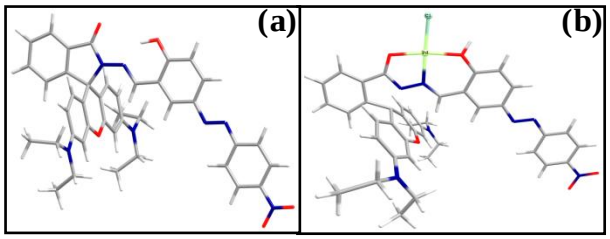

Fig. 9 B3LYP optimized structure of (a) L and (b) **L**-Pd^{2+}.

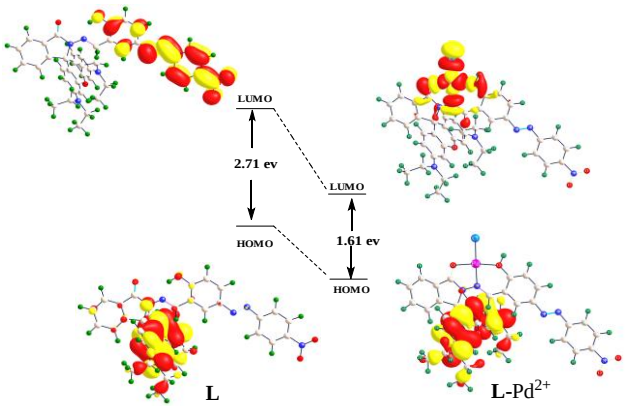

Fig. 10 HOMO and LUMO distributions of **L** and **L** -Pd^{2+}.

Due to the binding properties of **L** with Pd^{2+}, the **L**-Pd^{2+} complex showing intense emission in visible region essentially leads to its practical bio-imaging application. Nevertheless, to establish this fact it is a prerequisite to assess the cytotoxic effect of probe **L**, Pd^{2+}, and the complex on live cells. The MTT assay, which is based on mitochondrial dehydrogenase activity of viable cells, was adopted to study cytotoxicity of these compounds at varying concentrations as mentioned in experimental part. The probe **L** did not exert any adverse effect on cell viability, and the same is the case when cells were treated with varying concentrations of Pd^{2+}. The viability of Vero cells was not influenced by the amount of solvent (DMSO) which has been used for the experiment. Neither the Na_2S showed any detrimental effect in the concentration it has been applied for microscopic studies. The results obtained in the in vitro cytotoxic assay suggested that, in order to pursue confocal imaging studies of **L**-Pd^{2+} complex in live cells, we choose a working concentration of 1μM for probe compound. Thus to assess the effectiveness of compound **L** as a probe for intracellular detection of Pd^{2+} by confocal microscopy, Vero cells were treated with 100 μM $PdCl_2$ for 1 h followed by 1μM probe solution to promote formation of **L**-Pd^{2+} complex. Confocal microscopic studies revealed a lack of fluorescence for Verocells when treated with either probe compound or $PdCl_2$ alone (Fig.11, b and f). Upon incubation with $PdCl_2$ followed by probe **L**, striking switch-on fluorescence was observed inside Verocells, which indicated the formation of **L**-Pd^{2+} complex, as observed earlier in solution studies. Further, an intense red fluorescence was conspicuous in the perinuclear region of Vero cells (Fig. 11c). Interestingly, when the cells were treated with Na_2S solution (Fig. 11e) this bright red fluorescence significantly disappeared. The confocal microscopic analysis strongly suggested that probe **L** could readily cross the membrane barrier of the Vero cells, and rapidly sense intracellular Pd^{2+}. It is significant to mention here that bright field images of treated cells did not reveal any gross morphological changes, which suggested that Vero cells were viable. These findings open up the avenue for future in vivo biomedical applications of the sensor. Thus, **L** can be a suitable fluorescence chemosensing probe for $PdCl_2$ detection in biological systems.

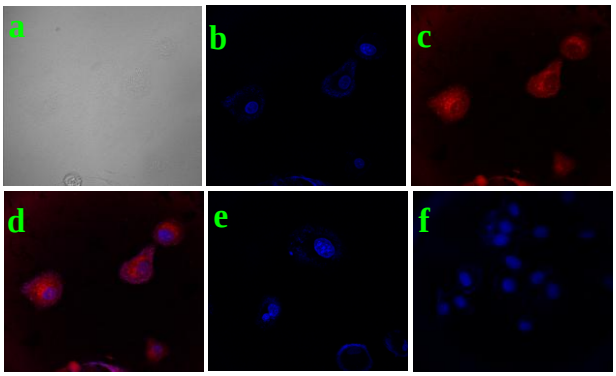

Fig. 11 Confocal microscopic images of probe in Vero 76 cells pretreated with $PdCl_2$: (a) bright field image of the cells, (b) only $PdCl_2$ at $1.0x10^{-4}$ M concentration, nuclei counterstained with DAPI (1 μg/mL), (c) stained with probe **L** at concentration $1.0x10^{-6}$ M, (d) overlay image in dark field, (e) cells treated with $PdCl_2$ at $1.0x10^{-4}$ M, probe at concentration 1.0 x 10^{-6} M and 4.0 x 10^{-5} M Na_2S, dimmed red signal is detected, and (f) cells treated only with probe at concentration 1.0 x 10^{-6} M, nuclei counterstained with DAPI (1 μg/mL), no background signal is detected. All images were acquired with a 60x objective lens. Scale bar represents 20 μm.

Conclusion

In conclusion, we have synthesized and characterized a new fluorescence turn-on Pd^{2+} probe, and the structure has been determined based on single crystal XRD. The probe exhibits large fluorescence enhancement, high selectivity, low detection limit, and fast response. The complex formation, stoichiometry, and binding mode have been established by UV−Vis, ESI-MS, and ^1H NMR studies and found to be 1:1. DFT calculation was carried out to demonstrate the electronic properties of **L** and the corresponding palladium complex. Furthermore, we have demonstrated that the probe is applicable for Pd^{2+} imaging in the living cells.

Experimental Section

General Information and Materials

The ^{1}H and ^{13}C NMR spectra were measured on Bruker–400 MHz spectrometer. Mass spectra were carried out using a Water's QTOF Micro YA 263 mass spectrometer. UV–visible and fluorescence spectra measurements were performed on a SHIMADZU UV-1800 and a Photon Technology International (PTI-LPS-220B) spectrofluorimeter respectively. FTIR spectra were recorded from their KBr pellets. Single crystal X-raydiffraction data for **L1** were collected on Bruker APEX II Duo CCD area-detector diffractometer at 294K temperature .

All cationic compound such as perchlorate of Mg^{2+}, Cu^{2+}, Fe^{2+}, Co^{2+}, Ni^{2+}, Mn^{2+}, chlorides of Li^{+}, Na^{+}, K^{+}, Ca^{2+}, Sr^{2+}, Ba^{2+}, Cr^{3+}, Cd^{2+},Fe^{3+}, Zn^{2+} , Hg^{2+}, Pb^{2+}, Hf^{4+}, Sn^{4+}, Pd^{2+}, Au^{3+}, Ru^{3+} , nitrate salts of Ag^{+}, Al^{3+}, potassium salts of Pt^{2+} , sodium salts of S^{2-} and di-sodiumsalts of EDTA were purchased from a commercial supplier, stored in a desiccators under vacuum containing self-indicating silica, and used without any further purification. For spectrophotometer measurements, EtOH (Spectrochem) and Elix Millipore water were used as solvents throughout all experiments.

Preparation of Test solution for UV-vis and fluorescence study

A stock solution of the probe **L (**4.0×10^{-5} M) was prepared in EtOH/H_2O (1:1, v/v). All experiments were carried out in EtOH – H_2O solution (EtOH : H_2O = 1 : 1, v/v, 10mM HEPES buffer, pH = 7.4). In titration experiments, each time a 4×10^{-5} M solution of **L** was filled in a quartz optical cell of 1 cm optical path length, and the ion stock solutions were added into the quartz optical cell gradually by using a micropipette. Spectral data were recorded at 1 min after the addition of the ions. In selectivity experiments, the test samples were prepared by placing appropriate amounts of the anions/cations (1×10^{-4} M) stock into 2 mL of solution of **L** (4×10^{-5} M).

Computational Studies. All geometries for **L** and **L**-Pd^{2+} were optimized by density functional theory (DFT) calculations using Gaussian 09 (B3LYP/6-31G(*d*,*p*)) software package.[25]

Cell Culture. Vero cell (very thin endothelial cell) (Vero 76, ATCC No CRL-1587) lines were prepared from continuous culture in Dulbecco's modified Eagle's medium (DMEM, Sigma Chemical Co., St. Louis, MO) supplemented with 10% fetal bovine serum (Invitrogen), penicillin (100 µg/mL), and streptomycin (100 µg/mL). The Vero 76 were obtained from the American Type Culture Collection (Rockville, MD) and maintained in DMEM containing 10% (v/v) fetal bovine serum and antibiotics in a CO_2 incubator. Cells were initially propagated in 75 cm^2 polystyrene, filter-capped tissue culture flask in an atmosphere of 5% CO_2 and 95% air at 37°C in CO_2 incubator. When the cells reached the logarithmic phase, the cell density was adjusted to $1.0x\ 10^5$ per/well in culture media. The cells were then used to inoculate in a glass bottom dish, with 1.0 mL ($1.0\ x\ 10^4$ cells) of cell suspension in each dish. After cell adhesion, culture medium was removed. The cell layer was rinsed twice with phosphate buffered saline (PBS), and then treated according to the experimental need.

Cell Imaging Study. For confocal imaging studies Vero cells, $1\ x10^4$ cells in 1000 µL of medium, were seeded on sterile 35 mm covered Petridis, glass bottom culture dish (ibidi GmbH, Germany), and incubated at 37°C in a CO_2 incubator for 10 hours. Then cells were washed with 500 µL DMEM followed by incubation with $1.0\ x10^{-4}$ M $PdCl_2$ dissolved in 500 µL DMEM at 37°C for 1 h in a CO_2 incubator and observed under an Olympus IX81 microscope equipped with a FV1000 confocal system using 1003 oil immersion Plan Apo (N.A. 1.45) objectives. Images obtained through section scanning were analyzed by Olympus Fluoview (version 3.1a; Tokyo, Japan) with excitation at 561 nm monochromatic laser beam, and emission spectra were integrated over the range 575-675 nm (single channel). The cells were again washed thrice with phosphate buffered saline PBS (pH 7.4) to remove any free $PdCl_2$ and incubated in PBS containing probe **L** to a final concentrations of $1.0\ x\ 10^{-6}$ M, incubated for 10 min followed by washing with PBS three times to remove excess probe outside the cells and images were captured. In a separate culture dish undergoing the same treatment the cells were then treated with $4.0\ x\ 10^{-5}$ M of Na_2S solution for 1 h; the cells were washed with PBS three times to remove free compound and ions before analysis. In separate culture dish the cells were similarly treated with $1.0\ X\ 10^{-6}$ M probe **L**, incubated for 10 min, washed thrice with PBS and the image was captured to get any possible background fluorescence. According to the need of the experiment we follow similar procedures to label the cell nuclei by treatment with DAPI (1 µg/mL) followed by three times wash with PBS and subsequently image was captured with excitation wavelength of laser was 405 nm, and emission was 461 nm. For all images, the confocal microscope settings, such as transmission density, and scan speed, were held constant to compare the relative intensity of intracellular fluorescence.

Cytotoxicity Assay. The cytotoxic effects of probe **L**, $PdCl_2$, and **L**-Pd^{2+}complex were determined by an MTT [3-(4,5-dimethylthiazol-2-yl)-2,5-diphenyltetrazolium bromide] assay following the manufacturer's instruction (MTT 2003, Sigma-Aldrich, MO). Vero cells were cultured into 96-well plates (10^4 cells per well) for 24 h. After overnight incubation, the medium was removed, and various concentrations of **L**, $PdCl_2$, and **L**-Pd^{2+} complex (0, 5, 25, 50, 75, and 100 µM) made in DMEM were added to the cells and incubated for 24 h. Control experiments were set with DMSO, cells without any treatment and cell-free medium were also included in the study. Following incubation, the growth medium was removed, and fresh DMEM containing MTT solution was added. The plate was incubated for 3−4 h at 37°C. Subsequently, the supernatant was removed, the insoluble colored formazan product was solubilized in DMSO, and its absorbance was measured in a microplate reader (Perkin-Elmer) at 570 nm. The assay was performed in triplicate for each concentration of **L**, $PdCl_2$, and **L**-Pd^{2+}. The OD value of wells containing only DMEM medium was subtracted from all readings to get rid of the background influence. The cell viability was

calculated by the following formula: (mean OD in treated wells / mean OD in control wells) X 100.

Synthesis of 1 and 2. Rhodamine-B hydrazide (**1**) and compound **2** were synthesized according to literature methods. [22]

Synthesis of chemosensor L. A mixture of compound **2** (0.250 g, 0.9 mmol) and Rhodamine B hydrazide (0.421 g, 0.9 mmol) in a 1:1 mixture of dry chloroform and absolute ethanol was refluxed for 12 h. After the completion of the reaction solvent was evaporated and the residue left was crystallized from EtOH to give compound **L** in 85% yield; M.P. > 250˚C. ^{1}H NMR (400 MHz, $CDCl_3$, $Si(CH_3)_4$, J (Hz), δ (ppm)): 11.62 (1H, s, -OH), 9.21(1H, s, -CH=N), 8.33 (2H, d, J=8.92 Hz), 7.99 (2H, d, J=7.00 Hz), 7.93 (1H, d, J=8.88 Hz), 7.85 (1H, dd, J=2.16 & 2.20 Hz), 7.79 (1H, d, J=2.20 Hz), 7.54 (2H, m), 7.18 (1H, d, J=7.12 Hz), 6.99 (1H, d, J=8.84 Hz), 6.50 (4H, d, J= 8.76 Hz), 6.27 (2H, dd, J= 2.44 & 2.46 Hz), 3.32 (8H, q, J=7.04 Hz, -N$\underline{CH_2}CH_3$), 1.15 (12H, t, J= 7.00 Hz, -NCH$_2\underline{CH_3}$). ^{13}C NMR ($CDCl_3$, 400 MHz) δ(ppm):=12.57,44.42,66.43,97.93,104.98,108.17,118.18,118.89,123.06,123.48,124.18,124.70,128.05,128.42, 128.68, 129.42, 129.11, 129.85, 133.78, 145.52, 148.19, 149.15, 150.75, 153.48, 155.90, 162.69, 164.46. TOF MS ES$^+$, m/z = 710.2786, calc. for $C_{41}H_{39}N_7O_5$ =709.8031.

Acknowledment

We thank the DST-West Bengal [Project no. 124(Sanc.)/ST/P/S&T/9G-17/2012] for financial support. SKM and SM thanks to the UGC, New Delhi for a fellowship and SKM also thanks Bhaskar Pramanik for his support. The authors (HKF) extend their appreciation to the Deanship of Scientific Research at King Saud University for funding this work through research group No. RGP-VPP-207.

Notes and references

[a]Department of Chemistry, Indian Institute of Engineering Science and Technology, Shibpur, Howrah-711103, West Bengal, India, Email: akmahapatra@rediffmail.com, Fax: +913326684564

[b] Institute of Chemistry, The Hebrew University of Jerusalem, 91904 Jerusalem, Israel.

[c] Department of Microbiology, University of Calcutta, Kolkata- 700019.

[d] X-ray Crystallography Unit, School of Physics, Universiti Sains Malaysia, 11800 USM, Penang, Malaysia.

[e] Department of Pharmaceutical Chemistry College of Pharmacy, King Saud University, P.O. Box. 2457, Riyadh 11451 Kingdom of Saudi Arabia.

† Electronic Supplementary Information (ESI) available: [details of any supplementary information available should be included here]. See DOI: 10.1039/b000000x/.

‡Crystal data for **L**: CCDC number-1013077. Emperical formula- $C_{41}H_{39}N_7O_5$. Molecular weight-709.79. Crystal system, space group- Triclinic, P1. Temperature (K)- 294. a, b, c (Å)- 10.244 (1), 13.8307 (14), 14.5665 (14). α, β, γ (°)-72.3415 (18), 70.1280 (18), 75.9246 (18). V (Å^3)- 1826.7 (3). Z – 2. Absorption coefficient (mm^{-1}) - 0.09. Crystal size (mm) - 0.62 × 0.27 × 0.11. No. of measured, independent and observed [I > 2σ(I)] reflections-21242, 6834, 4216. R [F^2 > 2σ(F^2)], wR(F^2), S-0.087, 0.291, 1.09. R_{int}.0.026.

1 (a) S. L. Buchwald, C. Mauger, G. Mignani and U. Scholzc, *Adv. Synth. Catal.*, 2006, **348**, 23; (b) X. Chen, K. M. Engle, D. H. Wang and J. Q. Yu, *Angew. Chem.*, 2009, **121**, 5196; (c) S. T. Omaye, *Toxicology*, 2002, **180**, 139; (d) S. L. Buchwald, C. Mauger, G. Mignani and U. Scholzc, *Adv. Synth. Catal.*, 2006, 348, 23.

2 (a) L. F. Tietze, H. Ila and H. P. Bell, *Chem. Rev.*, 2004, **104**, 3453; (b) H. F. Sore, W. R. J. D. Galloway and D. R. Spring, *Chem. Soc. Rev.*, 2012, **41**, 1845; (c) X. Wu, H. Neumann and M. Beller, *Chem. Soc. Rev.*, 2011, **40**, 4986.

3 K. Pyrzynska, *J. Environ. Monit.*, 2000, **2**, 99N.

4 M. Zischka, P. Schramel, H. Muntau, A. Rehnert, R. G. Gomez, B. Stojanik, G. Wannemaker, R. Dams, P. Quevauviller and E. A. Maier, T*rends Anal. Chem.* 2002, **21**, 851.

5 S. Zimmermann, F. Alt, J. Messerschmidt, A. V. Bohlen, H. Taraschewski and B. Sures, *Env iron. Toxicol. Chem.*, 2002, **21**, 2713.

6 M. Moldovan, S. Rauch, M. Go´mez, M. A. Palacios and G. M. Morrison, *Water Res.*, 2001, **35**, 4175.

7 D. S. Lee, *Nature*, 1983, **305**, 47.

8 (a) J. C. Wataha and C. T. Hanks, *J. Oral Rehabil.*, 1996, **23**, 309; (b) C. L. S. Wiseman and F. Zereini, *Sci. Total Environ.*, 2009, **407**, 2493; (c) T. Gebel, H. Lantzsch, K. Plebow and H. Dunkelberg, *Mutat. Res., Genet. Toxicol. Environ. Mutagen*, 1997, **389**, 183; (d) J. Kielhorn, C. Melber, D. Keller and I. Mangelsdorf, *Int. J. Hyg. Environ. Health*, 2002, **205**, 417.

9 J. C. Wataha and C. T. Hanks, *J. Oral Rehabil.*, 1996, **23**, 309.

10 International Programme on Chemical Safety, Palladium, Environmental Health Criteria Series 226, World Health Organization, Geneva, 2002.

11 (a) B. Dimitrova, K. Benkhedda, E. Ivanova and F. Adams, *J. Anal. At. Spectrom.*, 2004, **19**, 1394; (b) C. Locatelli, D. Melucci and G. Torsi, *Anal. Bioanal. Chem.*, 2005, **382**, 1567; (c) K. V. Meel, A. Smekens, M. Behets, P. Kazandjian and R. V. Grieken, *Anal. Chem.*, 2007, **79**, 6383.

12 (a) J. S. Kim and D. T. Quang, *Chem. Rev.*, 2007, **107**, 3780; (b) H. Li, J. Fan and X. Peng, *Chem. Soc. Rev*., 2013, **42**, 7943; (c) J. Du, M. Hu, J. Fan and X. Peng , *Chem. Soc. Rev.*, 2012, **41**, 4511; (d) A. K. Mahapatra, J. Roy, P. Sahoo, S. K. Mukhopadhyay and A. Chattopadhyay, *Org. Biomol. Chem.*, 2012, **10**, 2231; (e) A. K. Mahapatra, R. Maji, K. Maiti, S. S. Adhikari, C. D. Mukhopadhyay and D. Mandal, Analyst, 2014, **139**, 309.

13 (a) L. Fabbrizzi, M. Licchelli, P. Pallavicini, A. Perotti, A. Taglietti and D. Sacchi, *Chem.–Eur. J*., 1996, **2**, 75; (b) L. P. Duan, Y. F. Xu and X. H. Qian, *Chem. Commun.*, 2008, 6339.

14 T. Schwarze, H. Mu¨ ller, C. Dosche, T. Klamroth, W. Mickler, A. Kelling, H. G. Lo¨ hmannsro¨ ben, P. Saalfrank and H. J. Holdt, *Angew. Chem., Int. Ed.*, 2007, **46**, 1671.

15 Fluorescent chemosensors for the palladium species: (a) S. Goswami, D. Sen, N. K. Das, H. Fun and C. K. Quah, *Chem. Commun*., 2011, **47**, 9101; (b) H. Kim, K. -S. Moon, S. Shim and J. Tae, *Chem.–Asian J.*, 2011, **6**, 1987; (c) H. Li, J. Fan, J. Du, K. Guo, S. Sun, X. Liu and X. Peng, *Chem. Commun*., 2010, **46**, 1079; (d) H. Li, J. Fan, F. Song, H. Zhu, J. Du, S.Sun and X. Peng, *Chem.–Eur. J*., 2010, **16**, 12349; (e) T. Schwarze, C. Dosche, R. Flehr, T. Klamroth, H. -G. L€ohmannsr€oben, P. Saalfrank, E. Cleve, H. -J. Buschmanne and H. -J. Holdt, *Chem. Commun.*, 2010, 46, 2034; (f) D. Keum, S. Kim and Y. Kim, *Chem. Commun.*, 2014, **50**, 1268.

16 Fluorescent chemodosimeters for the palladium species: (a) F. L. Song, E. J. Carder, C. C. Kohler and K. Koide, *Chem. –Eur. J.*, 2010, **16**, 13500; (b) M. E. Jun and K. H. Ahn, *Org. Lett.*, 2010, **12**, 2790; (c) T. Schwarze, W. Mickler, C. Dosche, R. Flehr, T. Klamroth, H. -G. Lomannsroen, P. Saalfrank and H. -J. Holdt, *Chem. –Eur. J.*, 2010, **16**, 1819; (d) A. L. Garner, F. Song and K. Koide, *J. Am. Chem. Soc.*, 2009,

131, 5163; (e) A. L. Garner and K. Koide, *Chem. Commun.*, 2009, 86; (f) W. Chen, B. D. Wright and Y. Pang, *Chem. Commun.*, **2012**, **48**, 3824; (g) D. Keum, S. Kim and Y. Kim, *Chem. Commun.*, 2014, **50**, 1268.

17 (a) B. Liu, Y. Bao, F. Du, H. Wang, J. Tian and R. Bai, *Chem. Commun.*, 2011, **47**, 1731; (b) L. Duan, Y. Xu and X. Qian, *Chem. Commun.*, 2008, 6339; (c) J. R. Matthews, F. Goldoni, H. Kooijman, A. L. Spek, A. P. H. J. Schenning and E. W. Meijer, *Macromol. Rapid Commun.*, 2007, **28**, 1809; (d) A. Tamayo, L. Escriche, J. Casabo, B. Covelo and C. Lodeiro, *Eur. J. Inorg. Chem.*, 2006, 2997; (e) K. Kubo, Y. Miyazaki, K. Akutso and T. Sakurai, Heterocycles, 1999, **51**, 965.

18 (a) M. Santra, S. K. Ko, I. Shin and K. H. Ahn, *Chem. Commun.*, 2010, **46**, 3964; (b) A. L. Garner and K. Koide, *J. Am. Chem. Soc.*, 2008, **130**, 16472; (c) F. Song, A. L. Garner and K. Koide, *J. Am. Chem. Soc.*, 2007, **129**, 12354; (d) T. Schwarze, H. Muller, C. Dosche, T. Klamroth, W. Mickler, A. Kelling, H. -G. Lomannsroen, P. Saalfrank and H. -J. Holdt, *Angew. Chem., Int. Ed.*, 2007, **46**, 1671.

19 (a) S. Sun, B. Qiao, N. Jiang, J. Wang, S. Zhang and X. Peng, *Org. Lett.*, 2014, **16**, 1132; (b) B. Qiao, S. Sun, N. Jiang, S. Zhang and X. Peng, *Dalton Trans.*, 2014, **43**, 4626.

20 (a) X. Chen, T. Pradhan, F. Wang, J. S. Kim and J. Yoon, *Chem. Rev.*, 2012, **112**, 1910; (b) H. Li, H. Guan, X. Duan, J. Hu, G. Wang and Q. Wang, *Org. Biomol. Chem.*, 2013, **11**, 1805.

21 (a) M. E. Jun and K. H. Ahn, *Org. Lett.*, 2010, **12**, 2790; (b) H. Li, J. Fan, M. Hu, G. Cheng, D. Zhou, T. Wu, F. Song, S. Sun, C. Duan and X. Peng, *Chem.–Eur. J.*, 2012, **18**, 12242; (c) R. Balamurugan, C. Chien, K. Wu, Y. Chiu and J. Liu, *Analyst*, 2013, **138**, 1564; (d) S. Cai, Y. Lu, S. He, F. Wei, L. Zhao and X. Zeng, *Chem. Commun.*, 2013, **49**, 822; (e) A. K. Mahapatra, S. K. Manna, D. Mandal and C. D. Mukhopadhyay, *Inorg. Chem.*, 2013, **52**, 10825; (f) K. Ghosh, T. Sarkar and A. Samadder, *Org. Biomol. Chem.*, 2012, **10**, 3236.

22 (a) A. K. Mahapatra, S. K. Manna and P. Sahoo, *Talanta*, 2011, **85**, 2673; (b) V. Dujols, F. Ford and A. W. Czarnik, *J. Am. Chem. Soc.* 1997, **119**, 7386.

23 (a) O. Adeyi, W. B. Cross, G. Forrest, L. Godfrey, E. G. Hope, A. McLeod, A. Singh, K. Singh, G. A. Solan, Y. Wang and L. A. Wright, *Dalton Trans.*, 2013, **42**, 7710; (b) H. –X. Wang, Y. -H. Lang, H. -X. Wang, J. -J. Lou, H. -M. Guo and X. -Y. Li, *Tetrahedron*, 2014, **70**, 1997; (c) B. Calmuschi and U. Englert, C*ryst. Eng. Comm.*, 2005, **7**, 171; (d) S. Halder, M. G. B. Drew and S. Bhattacharya, *J. Chem. Sci.*, 2008, **120**, 441.

24 (a) A. D. Becke, *J. Chem. Phys.*, 1993, **98**, 5648; (b) C. Lee, W. Yang and R. G. Parr, *Phys. Rev. B*, 1988, **37**, 785; (c) D. Andrae, U. Haeussermann, M. Dolg, H. Stoll and H. Preuss, *Theor. Chim. Acta*, 1990, **77**, 123.

25 M. J. Frisch, G. W. Trucks, H. B. Schlegel, G. E. Scuseria, M. A. Robb, J. R. Cheeseman, G. Scalmani, V. Barone, B. Mennucci, G. A. Petersson, H. Nakatsuji, M. Caricato, X. Li, H. P. Hratchian, A. F. Izmaylov, J. Bloino, G. Zheng, J. L. Sonnenberg, M. Hada, M. Ehara, K. Toyota, R. Fukuda, J. Hasegawa, M. Ishida, T. Nakajima, Y. Honda, O. Kitao, H. Nakai, T. Vreven, J. A. Montgomery, Jr., J. E. Peralta, F. Ogliaro, M. Bearpark, J. J. Heyd, E. Brothers, K. N. Kudin, V. N. Staroverov, T. Keith, R. Kobayashi, J. Normand, K. Raghavachari, A. Rendell, J. C. Burant, S. S. Iyengar, J. Tomasi, M. Cossi, N. Rega, J. M. Millam, M. Klene, J. E. Knox, J. B. Cross,V. Bakken, C. Adamo, J. Jaramillo, R. Gomperts, R. E. Stratmann, O. Yazyev, A. J. Austin, R. Cammi, C. Pomelli, J. W. Ochterski, R. L. Martin, K. Morokuma, V. G. Zakrzewski, G. A. Voth, P. Salvador, J. J. Dannenberg, S. Dapprich, A. D. Daniels, O. Farkas, J. B. Foresman, J. V. Ortiz, J. Cioslowski, and D. J. Fox, Gaussian 09, Revision D.01, Gaussian, Inc., Wallingford CT, 2013.

Graphical Abstract

Azodye−Rhodamine-Based Fluorescent and Colorimetric Probe Specific for the Detection of Pd^{2+} in Aqueous Ethanolic Solution: Synthesis, XRD characterization, Computational Studies and Imaging in Live Cells

Ajit Kumar Mahapatra*, Saikat Kumar Manna, Kalipada Maiti, Sanchita Mondal, Rajkishor Maji, Debasish Mondal, Sukhendu Mandal, Md. Raihan Uddin, Shyamaprosad Goswami, Ching Kheng Quah and Hoong-Kun Fun

Azodye–rhodamine hybrid colorimetric fluorescent probe (**L**) has been designed and synthesized for selective *turn-on* fluorescence chemosensor for Pd^{2+}.